ESAIM: M2AN 51 (2017) 1303–1316
DOI: 10.1051/m2an/2016062

ESAIM: Mathematical Modelling and Numerical Analysis
www.esaim-m2an.org

A HYBRID TWO-STEP FINITE ELEMENT METHOD FOR FLUX APPROXIMATION: *A PRIORI* ESTIMATES

JaEun Ku[1], Young Ju Lee[2] and Dongwoo Sheen[3]

Abstract. We present a new two–step method based on the hybridization of mesh sizes in the traditional mixed finite element method. On a coarse mesh, the primary variable is approximated by a standard Galerkin method, whose computational cost is very low. Then, on a fine mesh, an $H(\mathrm{div})$ projection of the dual variable is sought as an accurate approximation for the flux variable. Our method does not rely on the framework of traditional mixed formulations, the choice of pair of finite element spaces is, therefore, free from the requirement of inf-sup stability condition. More precisely, our method is formulated in a fully decoupled manner, still achieving an optimal error convergence order. This leads to a computational strategy much easier and wider to implement than the mixed finite element method. Additionally, the independently posed solution strategy allows to use different meshes as well as different discretization schemes in the calculation of the primary and flux variables. We show that the finer mesh size h can be taken as the square of the coarse mesh size H, or a higher order power with a proper choice of parameter δ. This means that the computational cost for the coarse-grid solution is negligible compared to that for the fine-grid solution. In fact, numerical experiments show an advantage of using our strategy compared to the mixed finite element method. Some guidelines to choose an optimal parameter δ are also given. In addition, our approach is shown to provide an asymptotically exact *a posteriori* error estimator for the primary variable p in H^1 norm.

Mathematics Subject Classification. 65N30, 65N15.

Received December 7, 2014. Revised May 15, 2016. Accepted September 8, 2016.

1. Introduction

The purpose of this paper is to develop a very efficient and easy-to-implement finite element method for the approximation of the flux variable based on a system of first-order equations for second-order elliptic differential equations. It is well-known that if the standard mixed method is applied to the system, the pair of finite element spaces for the primary function and the flux variable should satisfy the discrete inf-sup condition, which limits

Keywords and phrases. Finite element method, elliptic problem, flux variable, mixed finite element.

[1] Department of Mathematics, Oklahoma State University, 401 Mathematical Sciences, Stillwater, OK 74078, USA. jku@math.okstate.edu

[2] Department of Mathematics, Texas State University, San Marcos, TX 78666, USA. yjlee@txstate.edu

[3] Department of Mathematics, Seoul National University, Seoul 08826, Korea. dongwoosheen@gmail.com

Article published by EDP Sciences

the choice of wide variety of finite element spaces to few available pairs. Moreover, the nature of saddle point problem for the mixed formulation narrows the applicability of efficient linear solvers.

The main purpose of this work is to propose a new method which does not require the inf-sup condition and any conforming finite element spaces can be used for approximation spaces for the primary and flux(dual) variables. Some relevant works can be found at [10, 18].

Our main motivation is to obtain the approximate solutions for the flux variable accurately. The flux variable is the quantity of interest in many engineering applications: see [1, 3, 13, 16, 20] and the references therein. For an efficient computation of the flux variable, a simple but important observation in this paper is that we can obtain an approximate solution for the primary function on a coarse mesh and use it to obtain the approximate solutions for the flux variable on a finer mesh. Therefore, our method is built upon a two-grid procedure. Namely, in the first stage, we use the standard Galerkin method on a very coarse mesh to obtain an approximate the primary variable p, denoted by $p_H G$ In the second stage, we apply a finite element method on a finer mesh to obtain an approximate solution $\mathbf{u}_h$ for the flux variable $\mathbf{u}(= -\mathcal{A}\nabla p)$ using p_H^G.

We show that optimal convergence for the flux variable can be achieved by using the target mesh size h for the finer mesh while the coarse mesh can still be quite coarse. The typical case corresponds to the choice $\delta = 1$ in (2.6), and in this case our analysis shows that if p_H^G is found from the piecewise linear finite element and $\mathbf{u}_h$ is found from the lowest-degree Raviart−Thomas mixed finite element space, then H can be chosen as large as $h^{1/2}$, still preserving optimal convergence. Moreover, by choosing a parameter δ small, the ratio between the coarse mesh H and fine mesh h could be larger. For smaller δ, the computational cost for the primary variable is negligible while the resulting algebraic equation becomes closer to a singular system.

The solution to the system defined on a finer mesh can be obtained very efficiently by using well-known efficient multi-grid solvers for the $H(\mathrm{div})$ projection. A classical geometric multi-grid method has been proposed by Arnold, Falk and Winther [2]. More recently Hiptmair and Xu [17] proposed an auxiliary space preconditioner for the $H(\mathrm{div})$ system, which can be efficiently applied to the algebraic multi-grid methods [4].

Numerically, our method is shown to be comparable or outperform that from the mixed finite element method in accuracy while keeping total degrees of freedom lower than those of the mixed finite element method. Namely, while keeping the computational cost for the coarse-grid solution negligible compared to that for the fine-grid solution, we can achieve a highly accurate flux variable. For example, when Brezzi−Douglas−Marini type elements are used, our method clearly outperforms the mixed finite element method; see Table 4 in Section 6.

Furthermore, similarly to the least-squares method applied to first-order systems, our method has a built-in *a posteriori* error estimators. The *a posteriori* error estimator has a very similar structure to the one developed for the least-squares method in [11]. We show that our error estimator is an asymptotically exact *a posteriori* error estimator; *i.e.* the ratio of true error and the estimator converges to 1 as the underlying mesh size converges to 0.

Previously, the flux variable is obtained by using postprocessing similar to our approach, *i.e.* [12]. Their goal was a construction of (recovery type) *a posteriori* error estimators, and the primary and flux variables are obtained on the same meshes. Our motivation is different from that of [12] in the following sense. Our goal is obtaining an accurate approximation for the flux variable and we use much finer meshes for the approximation of the flux variable compared to the ones for the primary variable. As a by-product, we obtain asymptotically exact *a posteriori* error estimators for the primary variable.

The rest of the paper is organized as follows. Section 2 introduces mathematical equations for the second-order elliptic equations and the $H(\mathrm{div})$ least-squares formulation is described for the equations. In Section 3, finite element spaces are introduced and our parameter-dependent two-step hybrid finite element method is defined. In Section 4, we establish an error estimate for $\|\mathbf{u} - \mathbf{u}_h\|_0$ by establishing a super-closeness of $\mathbf{u}_h$. We also give some guidelines to choose optimal parameter δ. In Section 5, superconvergence of $\mathbf{u}_h$ to the interpolant $\boldsymbol{\Pi}_h\mathbf{u}$ is discussed. Also we develop an equivalent a posterior error estimator for $\|\mathcal{A}^{1/2}\nabla(p - p_h)\|_0$. In Section 6, we present numerical examples confirming the theoretical results in this paper.

2. Parameter-dependent hybrid two-step formulation

Let Ω be a bounded domain in $\mathbb{R}^d, d = 2, 3$, with boundary $\partial\Omega$ and $\mathcal{A}$ be a $d \times d$ symmetric and uniformly positive definite matrix. For $f \in H^{-1}(\Omega)$ and $g \in H^{\frac{1}{2}}(\partial\Omega)$, we are interested in the approximation of the flux $\mathbf{u} = -\mathcal{A}\nabla p$ where the primary variable p fulfills the elliptic boundary value problem:

$$-\nabla \cdot (\mathcal{A}\nabla p) = f \quad \text{in} \quad \Omega, \qquad p = g \quad \text{on} \quad \partial\Omega. \tag{2.1}$$

Let $\widetilde{p} \in H^1(\Omega)$ be an extension of g to Ω. Then a weak form equivalent to (2.1) is to find $p \in H^1(\Omega)$ such that $p - \widetilde{p} \in H_0^1(\Omega)$ fulfilling

$$(\mathcal{A}\nabla p, \nabla q) = (f, q) + (\mathcal{A}\nabla \widetilde{p}, \nabla q) \quad \forall\, q \in H_0^1(\Omega). \tag{2.2}$$

We assume that the domain Ω and the coefficient $\mathcal{A}$ are sufficiently smooth such that, for $f \in H^{r-1}(\partial\Omega)$ and $g \in H^{r-\frac{1}{2}+\alpha}(\partial\Omega)$ for some integer $r \geq 1$ and $\alpha \in (0, 1]$, the unique solution $p \in H_0^1(\Omega)$ belongs to $H^{r+\alpha}(\Omega)$. Here, and in what follows, $H^s(K)$ and $H_0^s(K)$ denote the Sobolev spaces of order s defined on K with norm $\|\cdot\|_{s,K}$ and inner-product $(\cdot,\cdot)_{s,K}$. In case $K = \Omega$, we employ the convention to omit Ω from the subindex; moreover, the subscript s will be dropped if $s = 0$.

The flux variable can be well-approximated by the standard mixed formulation:

$$\mathcal{A}^{-1}\mathbf{u} + \nabla p = 0 \qquad \text{in } \Omega, \tag{2.3a}$$
$$\nabla \cdot \mathbf{u} = f \qquad \text{in } \Omega, \tag{2.3b}$$
$$p = g \qquad \text{on } \partial\Omega. \tag{2.3c}$$

Set

$$\mathbf{V} = H(\mathrm{div};\, \Omega) \quad \text{and} \quad W = L^2(\Omega), \quad \mathbb{M} = \mathbf{V} \times W,$$

where $H(\mathrm{div};\, K) = \{\mathbf{v} \in (L^2(K))^d : \nabla \cdot \mathbf{v} \in L^2(K)\}$, with norm $\|\mathbf{v}\|^2_{H(\mathrm{div};\, K)} = (\nabla \cdot \mathbf{v}, \nabla \cdot \mathbf{v})_K + (\mathbf{v}, \mathbf{v})_K$. Often we will use the following notation:

$$\|\mathbf{v}\|^2_{H(\mathrm{div};\, K, \mathcal{A}^{-1})} = (\nabla \cdot \mathbf{v}, \nabla \cdot \mathbf{v})_K + \left(\mathcal{A}^{-1}\mathbf{v}, \mathbf{v}\right)_K \quad \forall\, \mathbf{v} \in H(\mathrm{div};\, K).$$

Since $\mathcal{A}$ is uniformly positive definite, we have

$$c\|\mathbf{v}\|_{H(\mathrm{div};\, K)} \leq \|\mathbf{v}\|_{H(\mathrm{div};\, K, \mathcal{A}^{-1})} \leq C\|\mathbf{v}\|_{H(\mathrm{div};\, K)} \quad \forall \mathbf{v} \in H(\mathrm{div};\, K). \tag{2.4}$$

The standard mixed weak formulation of (2.3) is then to find $(\mathbf{u}, p) \in \mathbb{M} = \mathbf{V} \times W$ such that

$$(\mathcal{A}^{-1}\mathbf{u}, \mathbf{v}) - (p, \nabla \cdot \mathbf{v}) = -\langle g, \boldsymbol{\nu} \cdot \mathbf{v}\rangle_{\partial\Omega} \quad \forall\, \mathbf{v} \in \mathbf{V}, \tag{2.5a}$$
$$(\nabla \cdot \mathbf{u}, q) = (f, q) \quad \forall\, q \in W. \tag{2.5b}$$

It is well-known that the above mixed formulation (2.5) is a saddle point problem and it requires certain cares to adopt a suitable pair of finite element spaces and stable numerical solvers. For this reason we seek a different approach from the classical mixed finite element method.

Instead of approximating (2.5) directly, we propose an approach by a parameter–dependent hybrid mixed formulation by adding δ times (2.5a) to (2.5b) with the choice of $q = \nabla \cdot \mathbf{v}$:

$$(\nabla \cdot \mathbf{u}, \nabla \cdot \mathbf{v}) + \delta(\mathcal{A}^{-1}\mathbf{u}, \mathbf{v}) = (f + \delta p, \nabla \cdot \mathbf{v}) - \delta\, \langle g, \boldsymbol{\nu} \cdot \mathbf{v}\rangle_{\partial\Omega}. \tag{2.6}$$

Our hybrid numerical approximation scheme is composed of two steps, based on (2.2) and (2.6) on two grids of size H and h with $0 < h \leq H < 1$.

Step 1. Obtain a coarse-grid solution p_H^G which approximates p of (2.2);
Step 2. Utilizing p_H^G, find a fine-grid solution $\mathbf{u}_h$ which approximates $\mathbf{u}$ of (2.6).

3. Two-step hybrid finite element approximation

In this section we review in brief some preliminaries on the classical mixed finite element spaces as these will be the motivation of our approach. Utilizing mixed finite element spaces, our parameter-dependent two-step hybrid finite element method will be introduced.

Let $(\mathscr{T}_h)_{0<h\leq 1}$ be a family of shape regular triangulations of Ω (see [7]) by triangular/tetrahedral or rectangular elements, where $h = \max_{K\in\mathscr{T}_h} h_K$, $h_K = \mathrm{diam}(K)$.

3.1. Preliminaries on the classic mixed finite element spaces

Denote by $\mathbb{RT}_h^{(k)}, k \geq 0$, and $\mathbb{BDM}_h^{(k)}, k \geq 1$, the Raviart−Thomas or Nedelec space [21, 22] and the Brezzi−Douglas−Marini or Brezzi–Douglas–Duran–Fortin space of index k [8,9] defined as follows:

$$\begin{cases} \mathbb{RT}_h^{(k)} := \{\mathbf{v}\in\mathbf{V} \,:\, \mathbf{v}|_K \in [P_k(K)]^d \oplus \mathrm{Span}\{\mathbf{x}P_k(K)\},\ K\in\mathscr{T}_h\}, \\ \mathbb{BDM}_h^{(k)} := \{\mathbf{v}\in\mathbf{V} \,:\, \mathbf{v}|_K \in [P_k(K)]^d, \quad K\in\mathscr{T}_h\}, \end{cases}$$

where $P_k(K)$ denotes the space of all polynomials up to degree k defined on K. Denote by $C^0(P_h^{(k)})$ the standard C^0-conforming finite element space of piecewise polynomials of degree $\leq k$ on mesh $\mathscr{T}_h$. We also designate by "$C^{-1}(P_h^{(k)})$" the space of piecewise polynomials of degree $\leq k$ on mesh $\mathscr{T}_h$, namely, $C^{-1}(P_h^{(k)}) = \{q\in L^2(\Omega)\colon q|_K \in P_k(K),\ K\in\mathscr{T}_h\}$.

Then the family of RTN/BDM-BDDF mixed finite element spaces of index $\iota(k), k = 0, 1, \ldots,$ are given by

$$\mathbb{M}_h^{(k)} := \mathbf{V}_h^{(k)} \times W_h^{(k)} := \begin{cases} \mathbb{RT}_h^{\iota(k)} \times C^{-1}(P_h^{(k)}), \\ \mathbb{BDM}_h^{\iota(k)} \times C^{-1}(P_h^{(k)}). \end{cases}$$

where

$$\iota(k) = \begin{cases} k, & \text{if } \mathbf{V}_h^{(k)} = \mathbb{RT}_h^{\iota(k)}, \\ k+1, & \text{if } \mathbf{V}_h^{(k)} = \mathbb{BDM}_h^{\iota(k)}. \end{cases}$$

Denote by $\boldsymbol{\Pi}_h \times P_h : \mathbf{V}\times W \to \mathbf{V}_h^{(k)} \times W_h^{(k)}$ the RTN/BDM-BDDF projection operator fulfilling the following commutativity property:

$$\nabla\cdot\boldsymbol{\Pi}_h = P_h\nabla\cdot : \mathbf{V} \xrightarrow{\text{onto}} W_h^{(k)}, \tag{3.1}$$

where $P_h : W \to W_h^{(r)}$ is the L^2-projection from W to $W_h^{(r)}$ such that

$$(p - P_h p, q_h) = 0, \quad q_h \in W_h^{(r)}, \quad p\in W. \tag{3.2}$$

The following estimates are valid [9], ([14], p. 41), ([9], p. 221), ([8], p. 241) ([21], p. 330):

$$\|q - P_h q\|_{-s} \leq C\left(\sum_{K\in\mathscr{T}_h} h_K^{2(r+s)}\|q\|_{r,K}^2\right)^{\frac{1}{2}}, \ 0\leq r,s\leq k+1, \tag{3.3a}$$

$$\|\mathbf{v} - \boldsymbol{\Pi}_h\mathbf{v}\|_0 \leq C\left(\sum_{K\in\mathscr{T}_h} h_K^{2r}\|\mathbf{v}\|_{r,K}^2\right)^{\frac{1}{2}}, \ 0\leq r\leq \iota(k)+1, \tag{3.3b}$$

$$\|\nabla\cdot(\mathbf{v} - \boldsymbol{\Pi}_h\mathbf{v})\|_{-s} \leq C\left(\sum_{K\in\mathscr{T}_h} h_K^{2(r+s)}\|\nabla\cdot\mathbf{v}\|_{r,K}^2\right)^{\frac{1}{2}}, \ 0\leq r,s\leq k+1, \tag{3.3c}$$

Here, and in what follows, we use C to denote a generic positive constant, which is independent of the mesh size h.

The mixed finite element approximation (2.5) is then to find $(\mathbf{u}_h^M, p_h^M) \in \mathbb{M}_h^{(k)}$ such that

$$(\mathcal{A}^{-1}\mathbf{u}_h^M, \mathbf{v}_h) - (p_h^M, \nabla\cdot\mathbf{v}_h) = -\langle g, \boldsymbol{\nu}\cdot\mathbf{v}_h\rangle_{\partial\Omega} \quad \forall\, \mathbf{v}_h \in \mathbf{V}_h^{(k)}, \tag{3.4a}$$

$$(\nabla\cdot\mathbf{u}_h^M, q_h) = (f, q_h) \quad \forall\, q_h \in W_h^{(k)}. \tag{3.4b}$$

Let $p_H^G \in C^0(P_H^{(r)})$ be the standard Galerkin approximation to p of (2.2) such that

$$(\mathcal{A}\nabla p_H^G, \nabla q_H) = (f, q_H) + (\mathcal{A}\nabla \widetilde{p}_H^G, \nabla q_H) \quad \forall\, q_H \in C^0(P_H^{(r)}), \tag{3.5}$$

where $\widetilde{p}_H^G$ denotes the $C^0(P_H^{(r)})$–interpolant of $\widetilde{p}$. Since p is $H^{r+\alpha}(\Omega)$–regular ($r \geq 1$), the following estimate holds:

$$\|p_H^G - p\|_0 + H^\alpha \|p_H^G - p\|_1 \leq CH^{2\alpha}|p|_{1+\alpha}. \tag{3.6}$$

Although $\mathbb{BDM}_h^{(k)}$ lies between $\mathbb{RT}_h^{(k-1)}$ and $\mathbb{RT}_h^{(k)}$, the vector-valued approximate solution by $\mathbb{BDM}_h^{(k)}$ is asymptotically of same convergent rate as that obtained by $\mathbb{RT}_h^{(k)}$; moreover, the scalar-valued approximate solution by $\mathbb{BDM}_h^{(k)}$ is asymptotically of same convergence as that employed by $\mathbb{RT}_h^{(k)}$ once a standard hybridization procedure is applied [8, 9]. For instance, the solution $\tilde{p}_h^{(0)}$ obtained by using the $\mathbb{M}_h^{(0)} = \mathbb{BDM}_h^{(0)} \times W_h^{(0)}$ with hybridization fulfills $\|p - \tilde{p}_h^{(0)}\|_0 \leq Ch^{2\alpha}\|p\|_{1+\alpha}$.

3.2. Parameter-dependent two-step hybrid finite element method

We propose a new two-step hybrid finite element method to approximate the flux variable in a mixed formulation setting, relaxing the constraint on the pair of mixed finite element spaces. First, the standard Galerkin method is applied on *a coarse mesh* $\mathscr{T}_H$, to obtain an approximate solution p_H^G. Then, by using p_H^G, an approximate flux variable $\mathbf{u}_h$ is obtained on *a finer mesh* $\mathscr{T}_h$. We remark that h can be taken as $H^{1+\alpha}$ when lower-order approximation spaces are employed, *i.e.* $r = 1$ and $k = 0$. Thus, the computational cost to obtain p_H^G is negligible compared to that required on finer meshes. Moreover, in order to find approximate solutions on finer meshes, one can use any suitable fast solvers such as multigrid methods.

In this section, we will omit the superscript if no confusion arises; instead, we will stress the subscript which represent the size of mesh $\mathscr{T}_h$ and $\mathscr{T}_H$.

We will designate by $(\mathbf{u}_h, p_H^G) \in \mathbf{V}_h^{(k)} \widetilde{\times} C^0(P_H^{(r)})$ the solution of the following Steps 1 and 2 based on the hybrid spaces $\mathbf{V}_h^{(k)}$ and $C^0(P_H^{(r)})$ with parameter δ:

Step 1 (Coarse-grid solution). On a coarse mesh $\mathscr{T}_H$, obtain a standard Galerkin solution $p_H^G \in C^0(P_H^{(r)})$ satisfying (3.5).

Step 2 (Fine-grid solution). On a finer mesh $\mathscr{T}_h$, find the $H(\mathrm{div};\, \Omega, \mathcal{A}^{-1})$ projection $\mathbf{u}_h \in \mathbf{V}_h^{(k)}$ for the given data $f + \delta p_H^G$, *i.e.*

$$(\nabla\cdot\mathbf{u}_h, \nabla\cdot\mathbf{v}_h) + \delta(\mathcal{A}^{-1}\mathbf{u}_h, \mathbf{v}_h) = (f + \delta p_H^G, \nabla\cdot\mathbf{v}_h) - \delta\langle g, \boldsymbol{\nu}\cdot\mathbf{v}_h\rangle_{\partial\Omega} \quad \forall\, \mathbf{v}_h \in \mathbf{V}_h^{(k)}. \tag{3.7}$$

Remark 3.1. Plugging $q_h = \nabla\cdot\mathbf{v}_h \in W_h^{(k)}$ in (3.4b) and adding it to (3.4a), we have

$$(\nabla\cdot\mathbf{u}_h^M, \nabla\cdot\mathbf{v}_h) + \delta(\mathcal{A}^{-1}\mathbf{u}_h^M, \mathbf{v}_h) = (f + \delta p_h^M, \nabla\cdot\mathbf{v}_h) - \delta\langle g, \boldsymbol{\nu}\cdot\mathbf{v}_h\rangle_{\partial\Omega} \quad \forall\, \mathbf{v}_h \in \mathbf{V}_h^{(k)}. \tag{3.8}$$

Subtracting (3.7) from (3.8), we see that

$$\left(\nabla\cdot(\mathbf{u}_h^M - \mathbf{u}_h), \nabla\cdot\mathbf{v}_h\right) + \delta\left(A^{-1}(\mathbf{u}_h^M - \mathbf{u}_h), \mathbf{v}_h\right) = \delta\left(p_h^M - p_H^G, \nabla\cdot\mathbf{v}_h\right), \tag{3.9}$$

for all $\mathbf{v}_h \in \mathbf{V}_h^{(k)}$. Thus the differences $\mathbf{u}_h^M - \mathbf{u}_h$ and $\nabla\cdot(\mathbf{u}_h^M - \mathbf{u}_h)$ are tamed by the factor $\sqrt{\delta}$ and δ, respectively. Indeed, if $C^0(P_H^{(r)})$ is replaced by $W_h^{(k)}$, the differences $\mathbf{u}_h^M - \mathbf{u}_h$ and $\nabla\cdot(\mathbf{u}_h^M - \mathbf{u}_h)$ are zeroes since $p_h^M = p_H^G$ in this case. We will come back to this point in Theorem 4.2, which clarifies what the difference is.

Remark 3.2. Especially, if $\delta = 1$ and the two underlying meshes used to approximate both primary and flux variables are identical, our method reduces to the $H(\mathrm{div})$ recovery procedure of Cai and Zhang [12]. Our approach allows to take finer meshes to approximate the flux variables with optimal rate of convergence. This is due to our formulation using $(p_H^G, \nabla\cdot\mathbf{v}_h) - \langle g, \boldsymbol{\nu}\cdot\mathbf{v}_h\rangle_{\partial\Omega}$ instead of $-(\nabla p_H^G, \mathbf{v}_H)$ and the choice of δ.

Remark 3.3. The existence and uniqueness result of $\mathbf{u}_h$ in Step 2 is guaranteed by the Lax−Milgram lemma. Moreover, the resulting algebraic equations involve symmetric positive definite matrices and thus such systems can be solved efficiently by well-developed linear solvers. As mentioned earlier, fast multigrid solvers are available for computing the $H(\mathrm{div};\Omega,\mathcal{A}^{-1})$ projections (see, for example, [2,17]).

By subtracting (3.7) from (2.6) for $\mathbf{v}_h \in \mathbf{V}_h^{(k)}$, we obtain the following quasi-orthogonality property:

$$(\nabla\cdot(\mathbf{u}-\mathbf{u}_h), \nabla\cdot\mathbf{v}_h) + \delta(\mathcal{A}^{-1}(\mathbf{u}-\mathbf{u}_h), \mathbf{v}_h) = \delta(p - p_H^G, \nabla\cdot\mathbf{v}_h) \quad \forall\, \mathbf{v}_h \in \mathbf{V}_h^{(k)}. \tag{3.10}$$

Remark 3.4. It will be shown that h can be taken as H^2 when the lowest-order approximation spaces are used with an appropriate degree of polynomials for the approximation p_H^G to p. For example, $\mathbb{RT}_h^{(0)}$ can be combined with $C^0(P_H^{(1)})$ in order to obtain numerical solutions with optimal rate of convergence: see Remark 4.8.

4. Error analysis and guidelines for optimal choice of the parameter δ

In this section we analyze the errors of $(\mathbf{u}_h, p_j^G) \in \mathbf{V}_h^{(k)} \,\widetilde{\times}\, C^0(P_j^{(r)})$, which solve (3.5) and (3.7) with $j = h, H$, respectively. Based on optimal error estimates, we provide some guideline to choose optimal parameter values for δ.

The following lemma, slightly modified one from ([19], Thm. 4.1) is useful.

Lemma 4.1. *Let P_h be the (local) $L^2(\Omega)$-projection defined by (3.2). Then,*

$$\|P_h(p_h^M - p_h^G)\| \le Ch^\alpha\Big(\|\mathbf{u} - \boldsymbol{\Pi}_h\mathbf{u}\|_{H(\mathrm{div};\,\Omega)} + \|p - p_h^G\|_1\Big).$$

We are now in a position to state and prove the first of our main results.

Theorem 4.2. *For $k, r \ge 0$, let $(\mathbf{u}_h, p_j^G) \in \mathbf{V}_h^{(k)} \widetilde{\times} C^0(P_j^{(r)})$, be the solutions of (3.7) and (3.5) with $j = h, H$, respectively, and $(\mathbf{u}_h^M, p_h^M) \in \mathbb{M}_h^{(k)}$ the mixed finite element solution fulfilling (3.4). Then, the following estimate is valid:*

$$\|\mathbf{u}_h - \mathbf{u}_h^M\|_{H(\mathrm{div};\,\Omega)} \le C\sqrt{\delta}\left[h^\alpha\left(\|p - p_h^G\|_1 + \|\mathbf{u} - \boldsymbol{\Pi}_h\mathbf{u}\|_{H(\mathrm{div};\,\Omega)}\right) + H^\alpha\|p - p_H^G\|_1\right]. \tag{4.1}$$

Proof. Plugging $\mathbf{v}_h = \mathbf{u}_h^M - \mathbf{u}_h \in \mathbf{V}_h^{(k)}$ in (3.9), one sees that

$$\begin{aligned}
&\left(\nabla\cdot(\mathbf{u}_h^M - \mathbf{u}_h), \nabla\cdot(\mathbf{u}_h^M - \mathbf{u}_h)\right) + \delta\left(A^{-1}(\mathbf{u}_h^M - \mathbf{u}_h), (\mathbf{u}_h^M - \mathbf{u}_h)\right)\\
&\quad = \delta\left(p_h^M - p_H^G, \nabla\cdot(\mathbf{u}_h^M - \mathbf{u}_h)\right) = \delta\left(P_h(p_h^M - p_H^G), \nabla\cdot(\mathbf{u}_h^M - \mathbf{u}_h)\right)\\
&\quad \le \delta\|P_h(p_h^M - p_H^G)\|\,\|\nabla\cdot(\mathbf{u}_h^M - \mathbf{u}_h)\|.
\end{aligned}$$

Hence, one has

$$\|\nabla\cdot(\mathbf{u}_h^M - \mathbf{u}_h)\| \le \delta\|P_h(p_h^M - p_H^G)\|, \tag{4.2a}$$

$$\|\mathbf{u}_h^M - \mathbf{u}_h\| \le C\sqrt{\delta}\|P_h(p_h^M - p_H^G)\|. \tag{4.2b}$$

Now, the triangle inequality, $\|P_h q\|_0 \le \|q\|_0$, and (3.6) lead to

$$\begin{aligned}
\|P_h(p_h^M - p_H^G)\| &\le \|P_h(p_h^M - p_h^G)\| + \|P_h(p_h^G - p)\| + \|P_h(p - p_H^G)\|\\
&\le \|P_h(p_h^M - p_h^G)\| + \|p - p_h^G\| + \|p - p_H^G\|\\
&\le \|P_h(p_h^M - p_h^G)\| + C\left(h^\alpha\|p - p_h^G\|_1 + H^\alpha\|p - p_H^G\|_1\right).
\end{aligned} \tag{4.3}$$

An application of Lemma 4.1 to (4.3) combined with (4.2) shows (4.1). This completes the proof. □

We now have the second main result of this paper.

Theorem 4.3. *Let* $\mathbf{u}_h, p_j^G, j = h, H, \mathbf{u}_h^M$, *and* p_h^M *be as in Theorem 4.2. Then, we have*

$$\|\mathbf{u}_h - \mathbf{u}\| \le C\|\boldsymbol{\Pi}_h\mathbf{u} - \mathbf{u}\| + C\sqrt{\delta}\big[h^\alpha\left(\|p_h^G - p\|_1 + \|\nabla\cdot(\boldsymbol{\Pi}_h\mathbf{u} - \mathbf{u})\|\right) + H^\alpha\|p_H^G - p\|_1\big].$$

Proof. Using the triangle inequality, we have

$$\|\mathbf{u} - \mathbf{u}_h\| \le \|\mathbf{u} - \mathbf{u}_h^M\| + \|\mathbf{u}_h^M - \mathbf{u}_h\| \le \|\mathbf{u} - \boldsymbol{\Pi}_h\mathbf{u}\| + \|\mathbf{u}_h^M - \mathbf{u}_h\|.$$

Now, using Theorem 4.2 in the above inequality, we obtain the desired result. This completes the proof. □

The following result is an immediate consequence of Theorems 4.3 and (3.3). It can be used to determine the fine mesh size h in Step 2 with respect to the coarse mesh size H in Step 1.

Theorem 4.4. *Assume that the solution* $(\mathbf{u}, p) \in \mathbb{M}$ *to* (2.5) *belongs to* $H^{r-1+\alpha}(\Omega)\times H^{r+\alpha}(\Omega)$. *For* $\iota(k)+1 \le r$ *and* $\ell \le r$, *let* $(\mathbf{u}_h, p_H^G) \in \mathbf{V}_h^{(k)}\widetilde{\times}C^0(P_H^{(\ell)})$, *be the pair of solutions to* (3.7) *and* (3.5), *respectively. Assume that* $0 < \delta \le 1$. *Then, the following estimate is valid:*

$$\|\mathbf{u} - \mathbf{u}_h\| \le C\left[h^{\iota(k)+\alpha}(1 + \sqrt{\delta}h^{\alpha-1})\|\mathbf{u}\|_{\iota(k)+\alpha} + \sqrt{\delta}H^{\ell+2\alpha-1}\|p\|_{\ell+\alpha}\right]. \tag{4.4}$$

Moreover, if $\nabla\cdot\mathbf{u} \in H^{\iota(k)}(\Omega)$ *in addition, then one has*

$$\|\mathbf{u} - \mathbf{u}_h\| \le C\left[h^{\iota(k)+\alpha}\|\mathbf{u}\|_{\iota(k)+\alpha} + \sqrt{\delta}H^{\ell+2\alpha-1}\|p\|_{\ell+\alpha}\right]. \tag{4.5}$$

Proof. Under the stated assumptions, we estimate each term in the right side of Theorem 4.3 using (3.3) and the standard error estimate of Galerkin approximation as follows: for $0 \le \iota(k) + 1 \le r$ and $0 \le \ell \le r$,

$$\begin{aligned}
\|\mathbf{u} - \mathbf{u}_h\| &\le C\|\mathbf{u} - \boldsymbol{\Pi}_h\mathbf{u}\| + C\sqrt{\delta}\left[h^\alpha\left(\|p - p_h^G\|_1 + \|\nabla\cdot(\mathbf{u} - \boldsymbol{\Pi}_h\mathbf{u})\|\right) + H^\alpha\|p - p_H^G\|_1\right]\\
&\le Ch^{\iota(k)+\alpha}\|\mathbf{u}\|_{\iota(k)+\alpha} + C\sqrt{\delta}\left[h^{\ell+2\alpha-1}\|p\|_{\ell+\alpha} + h^{\iota(k)+2\alpha-1}\|\nabla\cdot\mathbf{u}\|_{\iota(k)-1+\alpha}\right]\\
&\quad + C\sqrt{\delta}H^{\ell+2\alpha-1}\|p\|_{\ell+\alpha}\\
&\le Ch^{\iota(k)+\alpha}\left[\|\mathbf{u}\|_{\iota(k)+\alpha} + \sqrt{\delta}h^{\alpha-1}\|\nabla\cdot\mathbf{u}\|_{\iota(k)-1+\alpha}\right] + C\sqrt{\delta}H^{\ell+2\alpha-1}\|p\|_{\ell+\alpha}\\
&\le Ch^{\iota(k)+\alpha}(1 + \sqrt{\delta}h^{\alpha-1})\|\mathbf{u}\|_{\iota(k)+\alpha} + C\sqrt{\delta}H^{\ell+2\alpha-1}\|p\|_{\ell+\alpha}.
\end{aligned}$$

This proves (4.4).

Under the additional assumption $\nabla\cdot\mathbf{u} \in H^{\iota(k)}(\Omega)$, in the above second line, the term $h^{\iota(k)+2\alpha-1}\|\nabla\cdot\mathbf{u}\|_{\iota(k)-1+\alpha}$ is replaced by $h^{\iota(k)+\alpha}\|\nabla\cdot\mathbf{u}\|_{\iota(k)}$. Then, invoking the assumption $0 < \delta \le 1$, trivial modifications in the above inequalities show (4.4). □

In Theorem 4.4, the following guideline of δ–choices is given.

Corollary 4.5. *Under the assumptions given in Theorem 4.4, further assume that* $\iota(k) \le \ell$. *Then an optimal choice for* δ *can be given as follows:*

$$\delta = \left(\frac{h^{\iota(k)+\alpha}}{H^{\ell+2\alpha-1} - h^{\iota(k)+2\alpha-1}}\right)^2, \tag{4.6}$$

and if, in addition $\nabla\cdot\mathbf{u} \in H^{\iota(k)+1}(\Omega)$,

$$\delta = \left(\frac{h^{\iota(k)+\alpha}}{H^{\ell+2\alpha-1}}\right)^2. \tag{4.7}$$

With these choices of δ, *we have the corresponding maximal convergence order*:

$$\|\mathbf{u} - \mathbf{u}_h\| \le Ch^{\iota(k)+\alpha}.$$

Proof. The value of δ in (4.6) is obtained by equating the two terms in (4.4), and by solving for δ. Similarly that in (4.7) follows by equating the terms (4.5). □

The following is an immediate consequence of the above result.

Corollary 4.6. *Under the assumptions given in Corollary 4.5, choose k and ℓ such that $\iota(k) = r-1$ and $\ell = r$. Then an optimal choice for δ are given as follows:*

$$\delta = \left(\frac{h^{r-1+\alpha}}{H^{r+2\alpha-1} - h^{r+2\alpha-2}} \right)^2,$$

and if, in addition, $\nabla \cdot \mathbf{u} \in H^{\iota(k)+1}(\Omega)$,

$$\delta = \left(\frac{h^{r-1+\alpha}}{H^{r+2\alpha-1}} \right)^2. \tag{4.8}$$

With these choices of δ the following optimal order convergence is expected:

$$\|\mathbf{u} - \mathbf{u}_h\| \leq C h^{r-1+\alpha}. \tag{4.9}$$

Remark 4.7. In order to approximate $\mathbf{u} \in H^\alpha(\Omega)$ and $p \in H^{1+\alpha}(\Omega)$ assuming that $\|\nabla \cdot \mathbf{u}\|_1 < \infty$. Using the RTN family, choose $k = 0$ and $\ell = 1$ to take the hybrid space $\mathbb{RT}_h^{(0)} \widetilde{\times} C^0(P_H^{(1)})$. Recall that $\iota(k) = 0$ in this case. Then from (4.4), one sees that h can be taken as H^2 to obtain an optimal order of convergence, $\mathcal{O}(h^\alpha)$ in the typical case $\delta = 1$ as stated in (4.9) and (4.8).

Remark 4.8. Assume that $\|\nabla \cdot \mathbf{u}\|_2 < \infty$. In order to approximate $\mathbf{u} \in H^2(\Omega)$ and $p \in H^3(\Omega)$ using the BDM/BDDF family, one can choose $k = 0$ and $\ell = 2$ to take the hybrid space $\mathbb{BDM}_h^{(1)} \widetilde{\times} C^0(P_H^{(2)})$. (Recall $\iota(0) = 1$ in this case). Then, it follows from (4.4) that h can be taken as $H^{3/2}$ to achieve an optimal convergence rate, $\mathcal{O}(h^2)$ with $\delta = 1$, as stated in (4.9) and (4.8).

Remark 4.9. Using RTN family with $k = 0$ and $\ell = 1$, to take the hybrid space $\mathbb{RT}_h^{(0)} \widetilde{\times} C^0(P_H^{(1)})$ ($\iota(k) = 0$ in this case), we consider to solve the problem defined on the L-shaped domain, in which $p \in H^{1+\alpha}(\Omega)$ with $\alpha = \frac{2}{3}$ and $\nabla \cdot \mathbf{u} = 0$. See Section 6.2. If $h = H^2$ is fixed, one can choose $\delta = 1$ for an optimal convergence rate $\mathcal{O}(h^\alpha)$, as stated in (4.9) and (4.8). These formulae suggest that if $h = H^4$, we choose $\delta = h^\alpha$ to get the same optimal convergence rate.

5. Applications

In this section, we present two applications of our error estimate. The results show that our new method inherits some of the desirable properties of the least-squares method and the mixed finite element method. In particular, our method inherits super-closeness from the mixed finite element method and *a posteriori* estimates from the least-squares method.

5.1. Asymptotically exact *a posteriori* error estimator

In what follows, we show that $\|\mathcal{A}^{-1/2}(\mathbf{u}_h + \mathcal{A}\nabla p_H^G)\|$ is an asymptotically exact *a posteriori* error estimator for $\|\mathcal{A}^{1/2}\nabla(p - p_H^G)\|$ under a mild condition. The estimator can be used in adaptive procedures for efficient computations of approximate solutions. Note that similar error estimators are used in [11], where the least-squares finite element method is considered. In this section, we fix $h = CH^2$, $\delta = 1$ and we use the lowest-order mixed finite element space pair, *i.e.* $\mathbb{RT}_h^{(0)} \widetilde{\times} C^0(P_h^{(1)})$. We only assume that p is $H^{1+\alpha}$–regular, for $1/2 < \alpha \leq 1$. To the best of our knowledge, our estimator is the first asymptotically exact *a posteriori* error estimator without assuming smoother solutions.

We first define a function $m(H)$ which satisfies the following inequality:

$$\|\mathcal{A}^{-1/2}(\mathbf{u}-\mathbf{u}_h)\| \leq m(H)\|\mathcal{A}^{1/2}\nabla(p-p_H^G)\|. \tag{5.1}$$

Remark 5.1. Theorem 4.4 with $h = CH^2$ implies $\|\mathcal{A}^{-1/2}(\mathbf{u}-\mathbf{u}_h)\| \simeq \mathcal{O}(h^\alpha) = \mathcal{O}(H^{2\alpha})$ for $p \in H^{1+\alpha}(\Omega)$. On the other hand, we have $\|\mathcal{A}^{1/2}\nabla(p-p_H^G)\| \simeq \mathcal{O}(H^\alpha)$. Thus, choosing $m(H) = CH^\alpha$, the inequality (5.1) is satisfied. Also, note that $m(H) \to 0$ as $H \to 0$.

Let

$$\mathcal{E}(\mathbf{u}_h) = \|\mathcal{A}^{-1/2}(\mathbf{u}_h + \mathcal{A}\nabla p_H^G)\|.$$

The following Theorem is standard, whose proof can be found in [11] for example. We provide the sketch of proof for completeness.

Theorem 5.2. *Let $m(H)$ be a function defined in (5.1), and H is sufficiently small. Then,*

$$\frac{1}{1+m(H)}\mathcal{E}(\mathbf{u}_h) \leq \|\mathcal{A}^{1/2}\nabla(p-p_H^G)\| \leq \frac{1}{1-m(H)}\mathcal{E}(\mathbf{u}_h).$$

Proof. Using the triangle inequality, (2.3a), and (5.1), we have

$$\begin{aligned}\|\mathcal{A}^{1/2}\nabla(p-p_H^G)\| &\leq \|\mathcal{A}^{1/2}\nabla(p-p_H^G) + \mathcal{A}^{-1/2}(\mathbf{u}-\mathbf{u}_h)\| + \|\mathcal{A}^{-1/2}(\mathbf{u}-\mathbf{u}_h)\| \\ &= \|\mathcal{A}^{-1/2}(\mathbf{u}_h + \mathcal{A}\nabla p_H^G)\| + \|\mathcal{A}^{-1/2}(\mathbf{u}-\mathbf{u}_h)\| \\ &\leq \|\mathcal{A}^{-1/2}(\mathbf{u}_h + \mathcal{A}\nabla p_H^G)\| + m(H)\|\mathcal{A}^{1/2}\nabla(p-p_H^G)\|.\end{aligned}$$

Thus, we have

$$(1-m(H))\|\mathcal{A}^{1/2}\nabla(p-p_H^G)\| \leq \|\mathcal{A}^{-1/2}(\mathbf{u}_h + \mathcal{A}\nabla p_H^G)\|.$$

This proves the upper bound. The lower bound can be obtained similarly. This completes the proof. □

5.2. Superconvergence

Here, we present a superconvergence result of $\mathbf{u}_h$ to $\boldsymbol{\Pi}_h\mathbf{u}$ as an elementary consequence of Theorem 4.2. We define that $\mathbf{u}_h \in \mathbf{V}_h^{(k)}$ is superconvergent with order θ_s if

$$\|\mathbf{u}_h - \boldsymbol{\Pi}_h\mathbf{u}\|_0 = \mathcal{O}(h^{k+1+\theta_s}),$$

where $\theta_s > 0$ and h^{k+1} is the optimal convergence rate for the approximation space $\mathbf{V}_h^{(k)}$ defined in (3.3).

We take advantage of the known superconvergence result of the mixed finite element solutions $\mathbf{u}_h^M$. There are rather severe restrictions in order to have a superconvergence result for $\mathbf{u}_h^M$. For example, the underlying mesh needs to be of uniform triangulation. Also, the known superconvergence results for the mixed finite element solutions assumes that the underlying true solutions belong to H^3-space. Hence, we take $\alpha = 1$ in the estimate of Theorem 4.2, i.e. we assume the true solution belongs to at least H^2-space. For more details we refer the reader to [5, 6, 15, 23] and references therein.

Theorem 5.3. *Assume that the mixed finite element solution $\mathbf{u}_h^M$ is superconvergent to $\Pi_h\mathbf{u}$ with order θ_s, for some $\theta_s > 0$. Let the mesh sizes h, H, and the parameter δ satisfy*

$$\sqrt{\delta}H^2 = h^{k+1+\theta_s}. \tag{5.2}$$

Then,

$$\|\mathbf{u}_h - \Pi_h\mathbf{u}\| = \mathcal{O}(h^{k+1+\theta_s}).$$

Proof. By the triangle inequality and Theorem 4.2 with (5.2), we have

$$\begin{aligned}\|\mathbf{u}_h - \boldsymbol{\Pi}_h\mathbf{u}\| &\le \|\mathbf{u}_h - \mathbf{u}_h^M\| + \|\mathbf{u}_h^M - \boldsymbol{\Pi}_h\mathbf{u}\| \\ &\le C(p)\sqrt{\delta}H^2 + \|\mathbf{u}_h^M - \boldsymbol{\Pi}_h\mathbf{u}\| \\ &\le C(p)h^{k+1+\theta_s} + \|\mathbf{u}_h^M - \boldsymbol{\Pi}_h\mathbf{u}\|.\end{aligned}$$

From this we can conclude that $\mathbf{u}_h$ is superconvergent with order θ_s if $\mathbf{u}_h^M$ is superconvergent with order θ_s under the condition (5.2). This completes the proof. □

Our numerical experiments in Section 6 with the choice of $k = 0$, $h = H^{3/2}$, and $\delta = 1$ on uniform meshes show the order of superconvergence a little higher than $\theta_s = \frac{1}{3}$. The corresponding results with the choice of $k = 0$, $h = H^2$, and $\delta = h$ on uniform meshes show the order of superconvergence a little higher than $\theta_s = \frac{1}{2}$; indeed, θ_s is nearly 1 (see Tab. 8). The theoretical investigation on this superconvergence behavior will be an interesting subject to be developed.

6. Numerical examples

In this section, we present sample results from numerical experiments to confirm our theoretical results as well as to demonstrate the effectivity and the robustness of our algorithm. The first example is a simple example for which the full regularity of the solution is given. The second example treats the case of corner singularity. In particular, the primary focus in this section is on investigating the effectiveness of theoretical choice of the coarse grid size H or the size of δ for an optimal convergence rate of the flux variable.

For all the numerical examples, in order to look at convergence behaviors closely, uniform meshes are used instead of adaptive meshes. Also a direct solver(superLU) is employed in solving linear systems and the 16-point quadrature rule is used on each triangle. On the other hand, the small parameter δ makes the system of equations nearly singular, for which round-off errors are observed to cause accuracy deterioration. In our numerical computation, we use defect corrections to overcome round-off errors. Namely, using a solution obtained by the direct solver, we obtain a residual and calculate correction by solving the system once more. The improved accuracy of the solution is reported in our numerical tables.

6.1. The case of full elliptic regularity

The first example is given as follows. The domain is taken as $\Omega = (0,1)^2$, and the following Dirichlet boundary value problem is considered:

$$-\Delta p = f \quad \text{in } \Omega \quad \text{with } p = 0 \quad \text{on } \partial\Omega,$$

where f is generated by the analytic solution $p(x,y) = \sin(\pi x)e^y(y^2-y)$. For this example, uniform triangulations of Ω are adopted in our numerical simulation (Fig. 1). The fine-grid approximation of the flux variable, $\mathbb{RT}_h^{(0)}$ and $\mathbb{BDM}_h^{(1)}$ spaces are employed, while $C^0(P_H^{(1)})$ and $C^0(P_H^{(2)})$ are adopted to calculate the coarse-grid Galerkin approximations, respectively.

Tables 1 and 3 show errors in the computation of the primary variable using both coarser- and finer-grid Galerkin methods, and those in the calculation of the flux variable applying the fine-grid $H(\mathrm{div};\Omega,\mathcal{A}^{-1})$-projection. Both mixed elements give optimal convergence rates in the approximation of the flux variable. An *a posteriori* error estimator has also been computed and it is shown to be asymptotically exact.

Table 2 shows numerical results with $\delta = h^2$, corresponding to the results with $\delta = 1$ in Table 1. The choice of parameter $\delta = h^2$ allows to use the approximation of p_H^G at the coarsest mesh level $H = 1/4$ as an input to compute the flux $\mathbf{u}_h$ up to $h = 1/1024$, still achieving optimal convergence. Table 4 also shows effectivity in using δ. Namely, by simply choosing $\delta = h^{4/3}$, without using the conforming P_2 finite element approximation p_H^G for the approximation of p at coarse levels (as shown in Tab. 3), we can achieve optimal convergence for the flux variable $\mathbf{u}_h$ using the conforming P_1 finite element approximation p_H^G for the approximation of p at coarse levels.

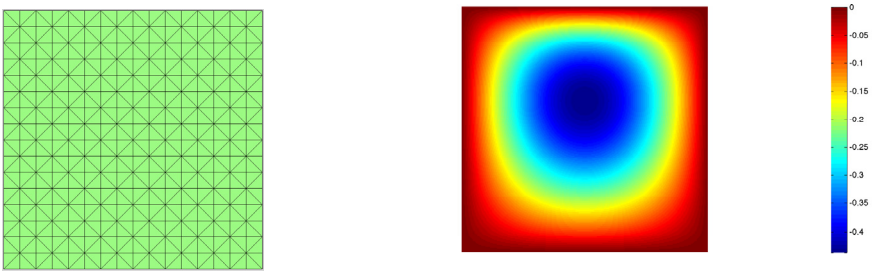

FIGURE 1. Typical uniform mesh used for triangulation of Ω, $H = 1/2^6$ and p_H^G.

TABLE 1. Errors and their reduction ratios of $(\mathbf{u}_h, p_H^G) \in \mathbb{RT}_h^{(0)} \widetilde{\times} C^0(P_H^{(1)})$; The parameter δ is chosen as 1.

$1/H$	$\lvert p - p_H^G\rvert_1$	$1/h$	$\lVert \mathbf{u} - \mathbf{u}_h\rVert$	Rate	$\lVert \mathbf{u}_h + \nabla p_H^G\rVert_0$	$\frac{\lVert \mathbf{u}_h + \nabla p_H^G\rVert_0}{\lvert p - p_H^G\rvert_1}$
4	0.405D+00	16	0.728D-01	×	0.407D+00	1.01
8	0.208D+00	64	0.183D-01	1.00	0.208D+00	1.00
16	0.105D+00	256	0.458D-02	1.00	0.105D+00	1.00
32	0.523D-01	1024	0.115D-02	1.00	0.523D-01	1.00

TABLE 2. Errors and their reduction ratios of $(\mathbf{u}_h, p_H^G) \in \mathbb{RT}_h^{(0)} \widetilde{\times} C^0(P_H^{(1)})$; The parameter δ is chosen as h^2.

$1/H$	$\lvert p - p_H^G\rvert_1$	$1/h$	$\lVert \mathbf{u} - \mathbf{u}_h\rVert$	Rate	$\lVert \mathbf{u}_h + \nabla p_H^G\rVert_0$	$\frac{\lVert \mathbf{u}_h + \nabla p_H^G\rVert_0}{\lvert p - p_H^G\rvert_1}$
4	0.405D+00	16	0.727D-01	×	0.410D+00	1.01
4	0.405D+00	64	0.182D-01	1.00	0.405D+00	1.00
4	0.405D+00	256	0.456D-02	1.00	0.405D+00	1.00
4	0.405D+00	1024	0.115D-02	0.99	0.405D+00	1.00

TABLE 3. Errors and their reduction ratios of $(\mathbf{u}_h, p_H^G) \in \mathbb{BDM}_h^{(1)} \widetilde{\times} C^0(P_H^{(2)})$; The parameter δ is chosen as 1.

$1/H$	$\lvert p - p_H^G\rvert_1$	$1/h$	$\lVert \mathbf{u} - \mathbf{u}_h\rVert$	Rate	$\lVert \mathbf{u}_h + \nabla p_H^G\rVert_0$	$\frac{\lVert \mathbf{u}_h + \nabla p_H^G\rVert_0}{\lvert p - p_H^G\rvert_1}$
4	0.686D-01	8	0.193D-01	x	0.693D-01	1.01
16	0.445D-02	64	0.311D-03	1.99	0.445D-02	1.00
64	0.279D-03	512	0.488D-05	2.00	0.279D-03	1.00

TABLE 4. Errors and their reduction ratios of $(\mathbf{u}_h, p_H^G) \in \mathbb{BDM}_h^{(1)} \widetilde{\times} C^0(P_H^{(1)})$; The parameter δ is chosen as $h^{4/3}$.

$1/H$	$\lvert p - p_H^G\rvert_1$	$1/h$	$\lVert \mathbf{u} - \mathbf{u}_h\rVert$	Rate	$\lVert \mathbf{u}_h + \nabla p_H^G\rVert_0$	$\frac{\lVert \mathbf{u}_h + \nabla p_H^G\rVert_0}{\lvert p - p_H^G\rvert_1}$
4	0.405D+00	8	0.197D-01	x	0.401D+00	0.99
16	0.105D+00	64	0.316D-03	1.99	0.105D+00	1.00
64	0.261D-01	512	0.498D-05	2.00	0.261D-01	1.00

TABLE 5. Comparisons of errors, their reduction ratios and DOFs between the hybrid and the RT mixed finite element solutions, $(\mathbf{u}_h, p_H^G) \in \mathbb{RT}_h^{(0)} \widetilde{\times} C^0(P_H^{(1)})$ and $(\mathbf{u}_h^M, p_h^M) \in \mathbb{RT}_h^{(0)} \times C^{-1}(P_h^{(0)})$. The parameter δ is chosen as 1.

$1/H$	$\|p - p_H^G\|$	$1/h$	$\|\mathbf{u} - \mathbf{u}_h\|$	DOF	$\|p - p_h^M\|$	$\|\mathbf{u} - \mathbf{u}_h^M\|$	DOF
4	0.40479D+00	16	0.72762D-01	841	0.4932D-01	0.72599D-01	1312
8	0.20784D+00	64	0.18305D-01	12 705	0.37350D-02	0.18243D-01	20 608
16	0.10446D+00	256	0.45801D-02	198 577	0.93379D-03	0.45622D-02	328 192

TABLE 6. Comparisons of errors, their reduction ratios and DOFs between the hybrid and the BDM mixed finite element solutions, $(\mathbf{u}_h, p_H^G) \in \mathbb{BDM}_h^{(1)} \widetilde{\times} C^0(P_H^{(2)})$ and $(\mathbf{u}_h^M, p_h^M) \in \mathbb{BDM}_h^{(1)} \times C^{-1}(P_h^{(0)})$. The parameter δ is chosen as 1.

$1/H$	$\|p - p_H^G\|$	$1/h$	$\|\mathbf{u} - \mathbf{u}_h\|$	DOF	$\|p - p_h^M\|$	$\|\mathbf{u} - \mathbf{u}_h^M\|$	DOF
4	0.68632D-01	8	0.19299D-01	817	0.30114D-01	0.31285D-01	544
16	0.44493D-02	64	0.31130D-03	35 121	0.37357D-02	0.50196D-03	33 024
64	0.27861D-03	512	0.48772D-05	1 757 233	0.46690D-03	0.78554D-05	2 099 200

TABLE 7. Superconvergence results for $\mathbf{u}_h$ to $\Pi_h \mathbf{u}$; the solution $\mathbf{u}_h$ is obtained using the hybrid space $\mathbb{RT}_h^{(0)} \widetilde{\times} C^0(P_H^{(1)})$. The parameter δ is chosen as 1.

$1/H$ for p_H^G	$1/h$	$\|\Pi_h \mathbf{u} - \mathbf{u}_h\|$	Rate
4	8	0.194D-01	×
16	64	0.510D-03	1.75
64	512	0.262D-04	1.43

Tables 5 and 6 demonstrate some comparison results between our method and the classical mixed finite element method. It is evident that the solution $(\mathbf{u}_h, p_H^G)$ obtained by using the hybrid space $\mathbb{BDM}_h^{(1)} \widetilde{\times} C^0(P_H^{(2)})$ converges faster than the solution $(\mathbf{u}_h^M, p_h^M)$ obtained by the classical mixed method $\mathbb{BDM}_h^{(1)} \times C^{-1}(P_h^{(0)})$ in both accuracy and efficiency considering the total degrees of freedom. On the other hand, accuracy in the approximation of the flux variable by using $\mathbb{RT}_h^{(0)} \widetilde{\times} C^0(P_H^{(1)})$ is comparable with that by using the standard mixed method by using $\mathbb{RT}_h^{(0)} \times C^{-1}(P_h^{(0)})$ while the hybrid approach uses less degrees of freedom than the latter.

Tables 7 and 8 show superconvergence results for the approximation of $\mathbf{u}_h$ using the hybrid space $\mathbb{RT}_h^{(0)} \widetilde{\times} C^0(P_H^{(1)})$. Numerical results in Table 7 with the choice of $k = 0$, $h = H^{3/2}$, and $\delta = 1$ on uniform meshes show the order of superconvergence a little higher than $\theta_s = \frac{1}{3}$. The corresponding results in Table 8 with the choice of $k = 0$, $h = H^2$, and $\delta = h$ on uniform meshes show the order of superconvergence much higher than $\theta_s = \frac{1}{2}$; indeed, θ_s is nearly 1.

Comparing the results for $1/h = 64$ in both tables, one sees that the numerical approximation with $\delta = h$ is much closer to the exact solution than that with $\delta = 1$, although a cheaper coarser-grid approximation to p_H^G in Table 8 is employed than the corresponding one in Table 7. This suggests to use $\delta = h$ instead of $\delta = 1$.

TABLE 8. Superconvergence results for $\mathbf{u}_h$ to $\Pi_h\mathbf{u}$; the solution $\mathbf{u}_h$ is obtained using the hybrid space $\mathbb{RT}_h^{(0)}\widetilde{\times}C^0(P_H^{(1)})$. The parameter δ is chosen as h.

$1/H$ for p_H^G	$1/h$	$\|\Pi_h\mathbf{u}-\mathbf{u}_h\|$	Rate
4	16	0.47095D-02	×
8	64	0.29624D-03	2.00
16	256	0.18515D-04	2.00
32	1024	0.12172D-05	1.96

This sort of observation can be found also for the numerical result for $1/H = 64, 1/h = 512$ in Table 7 and that for $1/H = 1, 1/h = 256$ in Table 8.

6.2. The case of partial elliptic regularity

We next consider (2.1) with constant coefficient in the non–convex domain $\Omega = (-1,1)^2 \setminus [0,1)\times(0,-1]$ with nonhomogeneous Dirichlet boundary data g. As an exact solution, the harmonic function $p(r,\theta) = r^\alpha \sin(\alpha\theta)$ is taken, where $\alpha = \frac{2}{3}$ so that $p \in H^{\frac{5}{3}}(\Omega)$ and $g \in H^{\frac{7}{6}}(\Gamma)$.

We approximate $(\mathbf{u}_h, p_H^G) \in \mathbb{RT}_h^{(0)}\widetilde{\times}C^0(P_H^{(1)})$ using uniform meshes. For the choices of δ, we attempted to use $\delta = 1$, 0.01 and a variable δ. A coarsest grid and a primary variable approximation on that grid, are given in Figure 2. The finest level grid used in this test, has the mesh size $h = 1/2^9$ while the coarsest level grid size is $H = 1/2^2$. If one wants to use the coarsest grid size for the primary variable to obtain an optimal L^2 convergence rate for the flux variable on the finest grid, then by (4.8), the theoretical δ should be chosen with $\alpha = \frac{2}{3}$ as follows:

$$\delta = \left(\frac{h}{H^2}\right)^{2\alpha} \approx 0.01.$$

We provide three results in Table 9, the computation of the flux variable, one obtained with $\delta = 1$, another with $\delta = 0.01$, and the other with $\delta = (h/H^2)^{2\alpha}$. We observe optimal L^2–convergence rates are achieved with both $\delta = 0.01$ and $\delta = (h/H^2)^{2\alpha}$ as shown in Table 9.

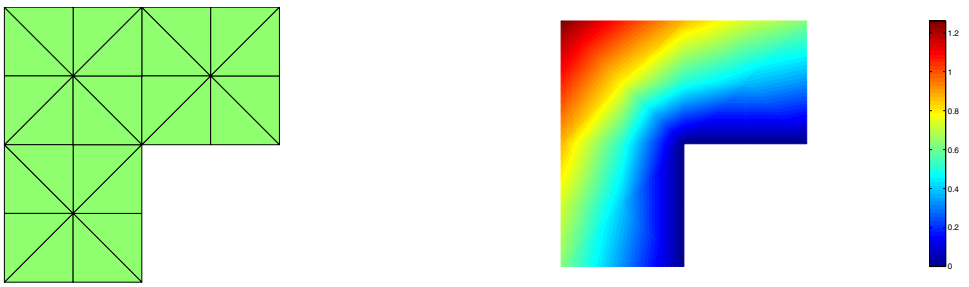

FIGURE 2. The mesh configuration used as $\mathscr{T}_H$ and the coarse grid solution p_H^G.

TABLE 9. Errors and their reduction ratios of $(\mathbf{u}_h, p_H^G) \in \mathbb{RT}_h^{(0)} \widetilde{\times} C^0(P_H^{(1)})$; The parameter δ is chosen as 1, 0.01, and $(h/H^2)^{2\alpha}$. The optimal convergence rate for the flux variable is $2/3 = 0.667$.

$1/H$	$\lvert p - p_H^G \rvert_1$	$1/h$	$\lVert \mathbf{u} - \mathbf{u}_h^1 \rVert$	Rate	$\lVert \mathbf{u} - \mathbf{u}_h^{0.01} \rVert$	Rate	$\lVert \mathbf{u} - \mathbf{u}_h^{(h/H^2)^{2\alpha}} \rVert$	Rate
4	0.116D+00	64	0.496D-01	×	0.491D-01	×	0.490D-01	×
4	0.116D+00	128	0.327D-01	0.600	0.311D-01	0.658	0.311D-01	0.658
4	0.116D+00	256	0.226D-01	0.536	0.197D-01	0.661	0.197D-01	0.661
4	0.116D+00	512	0.169D-01	0.421	0.124D-01	0.663	0.124D-01	0.663

Acknowledgements. The researches of Y.-J. Lee and D. Sheen were supported in part by NSF-DMS-1358953 and National Research Foundation of Korea (NRF–2014R1A2A1A11052429, and NRF–2015M3C4A7065662), respectively. The authors wish to thank the anonymous referees and the editor for their useful comments which led to a significant improvement of the paper.

REFERENCES

[1] T. Arbogast, M.F. Wheeler and I. Yotov, Mixed finite elements for elliptic problems with tensor coefficients as cell-centered finite differences. *SIAM J. Numer. Anal.* **34** (1997) 828–852.
[2] D.N. Arnold, R.S. Falk and R. Winther, Multigrid in $H(\mathrm{div})$ and $H(curl)$. *Numer. Math.* **85** (2000) 197–218.
[3] D. Boffi, F. Brezzi and M. Fortin, Mixed finite element methods and applications. Springer (2013).
[4] A. Brandt, Algebraic multigrid theory: The symmetric case. *Appl. Math. Comput.* **19** (1986) 23–56.
[5] J.H. Brandts, Superconvergence and a posteriori error estimation for triangular mixed finite elements. *Numer. Math.* **68** (1994) 311–324.
[6] J.H. Brandts, Superconvergence for triangular order $k = 1$ Raviart-Thomas mixed finite elements and for triangular standard quadratic finite element methods. *Appl. Numer. Math.* **34** (2000) 39–58.
[7] S.C. Brenner and L.R. Scott, The mathematical theory of finite element methods. Number 15 in *Texts in Applied Mathematics*. 2nd edition. Springer Verlag, New York (2002).
[8] F. Brezzi, J. Douglas Jr., R. Duran and M. Fortin, Mixed finite elements for second order elliptic problems in three variables. *Numer. Math.* **51** (1987) 237–250.
[9] F. Brezzi, J. Douglas, Jr. and L.D. Marini, Two families of mixed finite elements for second order elliptic problems. *Numer. Math.* **47** (1985) 217–235.
[10] M. Cai, M. Mu and J. Xu, Numerical solution to a mixed Navier-Sokes/Darcy model by the two-grid approach. *SIAM J. Numer. Anal.* **47** (2009) 3325–3338.
[11] Z. Cai, V. Carey, J. Ku and E.-J. Park, Asymptotically exact a posteriori error estimators for first-order div least-squares methods in local and global L_2 norm. *Comput. Math. Appl.* **70** (2015) 648–659.
[12] Z. Cai and S. Zhang, Flux recovery and a posteriori error estimators: Conforming elements for scalar elliptic equations. *SIAM J. Numer. Anal.* **48** (2010) 578–602.
[13] J. Douglas, Jr. and J.E. Roberts, Numerical methods for a model for compressible miscible displacement in porous media. *Math. Comput.* **41** (1983) 441–459.
[14] J. Douglas, Jr and J.E. Roberts, Global estimates for mixed methods for second order elliptic equations. *Math. Comput.* **44** (1985) 39–52.
[15] R.E. Ewing, M. Liu and J. Wang, A new superconvergence for mixed finite element approximations. *SIAM J. Numer. Anal.* **40** (2002) 2133–2150.
[16] V. Girault and P.A. Raviart, Finite Element Methods for Navier-Stokes equations. Theory and algorithm. Springer Verlag, Berlin (1986).
[17] R. Hiptmair and J. Xu, Nodal auxiliary space preconditioning in H(curl) and H(div) spaces. *SIAM J. Numer. Anal.* **45** (2007) 2483–2509.
[18] J. Jin, S. Shu and J. Xu, A two-grid discretization method for decoupling systems of partial differential equations. *Math. Comput.* **75** (2006) 1617–1626.
[19] J. Ku, Supercloseness of the mixed finite element method for the primary function on unstructured meshes and its applications. *BIT* **54** (2014) 1087–1097.
[20] Y.-J. Lee and J. Xu, New formulations, positivity preserving discretizations and stability analysis for non-Newtonian flow models. *Comput. Methods Appl. Mech. Engrg.* **195** (2006) 1180–1206.
[21] J. Nédélec, Mixed finite elements in R^3. *Numer. Math.* **35** (1980) 315–341.
[22] P. Raviart and J. Thomas, A mixed finite element method for 2nd order elliptic problems. In *Proc. of Conference on FEM held in Rome in 1975*. Vol. 606 of *Lect. Notes Math.* Springer Verlag (1977).
[23] J. Wang, Superconvergence and extrapolation for mixed element methods on rectangular domains. *Math. Comput.* **56** (1991) 477–503.